

Multi-class chronic lung disease classification based on guided backpropagation convolutional neural network using chest X-ray images

Rakesh Selva Raj¹, Pavan Kumar Madalu Palakshamurthy², Bidarakere Eswarappa Rangaswamy³

¹Department of Information Science and Engineering, Adichunchanagiri Institute of Technology, Chikkamagaluru, Visveswaraya Technological University, Belagavi, India

²Department of Information Science and Engineering, JNN College of Engineering, Shimoga, Visveswaraya Technological University, Belagavi, India

³Department of Academics, Visveswaraya Technological University, Belagavi, India

Article Info

Article history:

Received May 4, 2024

Revised Sep 20, 2024

Accepted Sep 30, 2024

Keywords:

Chest X-ray radiographic

Deep learning

EfficientNetB2

Gaussian filter

GBPCNN

ABSTRACT

Clinical diagnosis is crucial as chronic lung disease is a leading cause of mortality worldwide. Chest X-ray imaging is essential for the early and accurate diagnosis of lung diseases. However, due to the complexity of pathological abnormalities and detailed annotation, the computer-aided diagnosis of lung diseases is challenging. To overcome this challenge, this research proposes the guided backpropagation convolutional neural network (GBPCNN) for the classification of chronic lung disease into 14 classes, by adjusting the network's weights in CNN layers. The GBP technique enhances result accuracy by pinpointing the regions in an input image. Initially, the chest X-ray radiography (CXR) dataset is collected for estimating the effectiveness of the classifier. After collecting the dataset, the pre-processing is performed by utilizing image denoising using gaussian filter and normalization techniques. Then, the pre-processed data is fed to the feature extraction process, and it is done by using EfficientNetB2. Finally, extracted features are provided to the classification process to categorize chronic lung disease into 14 classes. The experimental results show that the proposed GBPCNN method attains better results and it achieves the accuracy of 97.94% as compared to the existing approaches like MobileLungNetV2 and CX-Ultranet. These results highlight the potential of our approach for clinical applications.

This is an open access article under the [CC BY-SA](https://creativecommons.org/licenses/by-sa/4.0/) license.



Corresponding Author:

Rakesh Selva Raj

Department of Information Science and Engineering, Adichunchanagiri Institute of Technology

Chikkamagaluru, Visveswaraya Technological University

Belagavi, India

Email: rakeshsr.cseng@gmail.com

1. INTRODUCTION

In this world, lung disease is one of the largest causes of cancer-related mortalities and it is the deadliest disease type [1]. Hence, early treatment and diagnosis can effectively minimize the life-threatening nature of lung disease as well as enhance the survival rate of cancerous people [2]. In the advanced medical image modalities, imaging tests are the most often utilized supportive modalities which can assist experts in diagnosing a range of illnesses [3]. There are various modalities utilized for diagnosing the various types of disease such as chest X-ray radiography (CXR), computed tomography (CT), mammogram, and histopathology [4]. Globally, CXR is the most performed radiology identification, and over 150 million

cancerous people have been identified annually in the United States with the help of this modality [5]. The infections of the lung in CXR images have been identified in the range of blunted costophrenic angles, cavitations, and so on. Hence, radiotherapists detect various situations of lung disease classes through the utilization of CXR images [6]. The classification and diagnosis of lung disease using CXR is such a difficult procedure for radiotherapists, because of the broad range of chest images [7]. Over the decade, the number of computer aided diagnosis (CAD) systems have been developed to use CXR images for the detection and classification of lung diseases [8]. However, these systems are unsuccessful in attaining the essential performance for the detection and classification of lung disease [9]. The researchers developed the deep learning (DL) approaches for attaining significant performance in the classification and detection [10]. The DL approaches can learn optimal features and ignore the additional feature extraction approaches [11]. The DL-based lung image classification approaches have attained efficient performance, particularly in CXR images [12], [13]. However, some previous approaches have been prone to imbalance problems, which become the most significant for lung image classification [14]. False positive rate (FPR), as well as false negative rates (FNR), leads to misclassification by including irrelevant or non-nodule regions as potential nodules [15].

To overcome this challenge, this research proposes the novel DL approach of guided propagation convolutional neural network (GPCNN) for the classification of lung disease. The guided propagation mainly considers the significant features and through propagating the data by the network based on guidance from previous layers, the GPCNN can efficiently capture the hierarchical features in lung images. In this section, recent research on chronic lung disease classification approaches based on CXR datasets is discussed. Shamrat *et al.* [16] presented the fine-tuned MobileLungNetV2 approach for the multi-class classification of lung disease from CXR images. The MobileLungNetV2 was obtained from the modification of the MobileNetV2. The CLAHE and data augmentation techniques were performed in the pre-processing step to obtain the contrast images and to enhance the input data. The gaussian filter was performed to denoise the noisy images. The MobileLungNetV2 had depth-wise separable convolutions as well as bottlenecks, so it minimized the number of input parameters from lung disease. However, this separation might restrict the capability of the model to intricate feature depictions. Souid *et al.* [17] developed the modified model MobileNet V2 approach for the prediction as well as classification of the lung pathologies of frontal thoracic X-rays. In the pre-processing stage, the data augmentation approach was performed to improve the input data. The classification was performed with the MobileNetV2 with the additional neural network (NN) layers. The MobileNetV2 model obtained better accuracy results. However, the recall of the model was relatively low compared to the other methods and it enhanced the false negative data classification in the prediction.

Wang *et al.* [18] introduced the triple-attention learning (A3 Net) for the classification of lung disease. The introduced approach utilized the pre-trained model of DenseNet-121 as the supportive network for the extraction of the feature. The A3 Net combined multiple attention mechanisms such as channel, element as well and scale-wise attention learning to capture the intricate details and learn hierarchical features in images. However, the introduced approach limited feature reuse when the image features were similar, so it caused poor classification performance. Kabiraj *et al.* [19] implemented the chest X-ray Ultranet (CX-Ultranet) for the classification and identification of 13 thoracic lung diseases from CXR. The CX-Ultranet utilized the multiclass cross-entropy loss function in a composite scaling approach with the help of EfficientNet for the extraction process. The suggested approach provided the maximum average results as well as effectively handled the class imbalance problem. However, the suggested approach failed to evaluate the region of interest (ROI) in input CXR, so it caused poor classification performance. Alshmrani *et al.* [20] presented the DL approach for the multiclassification of lung disease. The suggested approach has classified the disease into pneumonia, lung cancer, lung opacity as well as tuberculosis (TB). In the pre-processing step, the incredible CXR images were normalized as well as resized to enhance the model performance. The suggested approach utilized the pre-trained architecture of visual geometry group 19 (VGG19) which is performed through the help of CNN for the feature extraction as well as the FC network at the classification process. However, the suggested approach does not solve the overfitting problem. From this section, some limitations have been found: low recall value, overfitting, failure to evaluate the ROI in input data, poor classification performance, and limited feature reuse. To solve these problems, this research proposes the guided backpropagation convolutional neural network (GBPCNN) for the lung disease classification. The GBPCNN improves the feature representations by developing more informative features in lung disease. Detailed information about the proposed GBPCNN is discussed in the following section. The primary contributions of this research are noted in the following sections.

- The pre-processing is done by using two techniques: image denoising is performed through the gaussian filter to remove the noises through the exchange of every pixel's intensity with the weighted average of neighboring pixels to enhance the image quality. The data normalization is used to normalize the CXR

image data by normalizing the high and low values into 0 and 1. This approach supports enhancing the efficacy of the model by improving the learning capability in the lung disease classification.

- The feature extraction is done by using the pre-trained EfficientNetB2 architecture to extract meaningful features such as tumors and nodules from the CXR images. This approach makes the classifier effectively train the features.
- The DL approach of the GBPCNN classifier is proposed to classify chronic lung disease into 14 classes. It improves the feature representations by developing more informative features in lung disease. GBP makes sure that the CNN considers the features like size, texture, context as well as shape to effectively classify the data.

This paper is arranged as follows: section 2 provides the proposed methodology. Section 3 presents the classification using GBP using CNN. The results and discussion are provided in section 4 and section 5 gives the conclusion.

2. PROPOSED METHOD

This research proposes the classification of chronic lung disease into two categories such as benign and malignant by using GPCNN. This section comprises various steps: primarily, the data is collected by using CXR images. Then, pre-processing is performed by the image denoising and data normalization. After pre-processing, the features are extracted by using EfficientNetB2. Finally, classification is performed by using GPCNN for categorizing the 14 classes of chronic lung disease. Figure 1 shows the working steps of the proposed method.

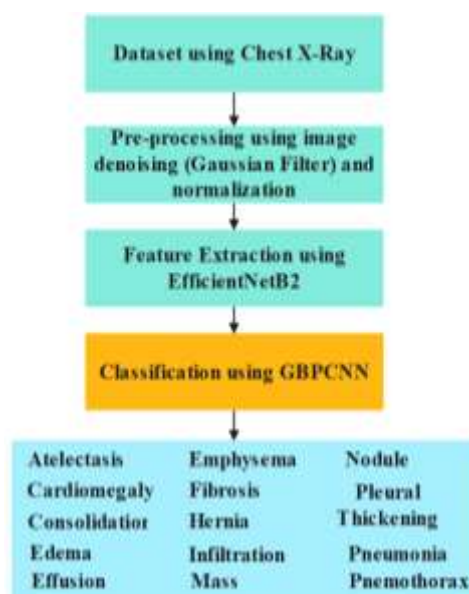


Figure 1. Workflow of the proposed method

2.1. Dataset collection

In this research, the CXR image dataset is considered to estimate the effectiveness of the proposed method. It is the publicly available dataset and it was acquired from Guangzhou Women and Children's Medical Center. This data involves the 112,120 bilateral thoracic X-ray data and the 60,412 normal data collected from 30,805 patients. Entire X-ray images were performed as part of the repetitive clinical care of the patients. This dataset involves 14 classes such as pneumonia, edema, emphysema, effusion, infiltration, mass, pleural thickening, pulmonary fibrosis, consolidation, pneumothorax, atelectasis, hernia, nodule and cardiomegaly [21]. This dataset image is stored in a PNG format with a size of 1024×1024 pixels. The collected dataset is fed to the pre-processing stage to achieve better classification performance. The pre-preprocessing is performed because the collected data contains unwanted noises, so it leads to poor performance. Figure 2 shows the sample images of the CXR image data.

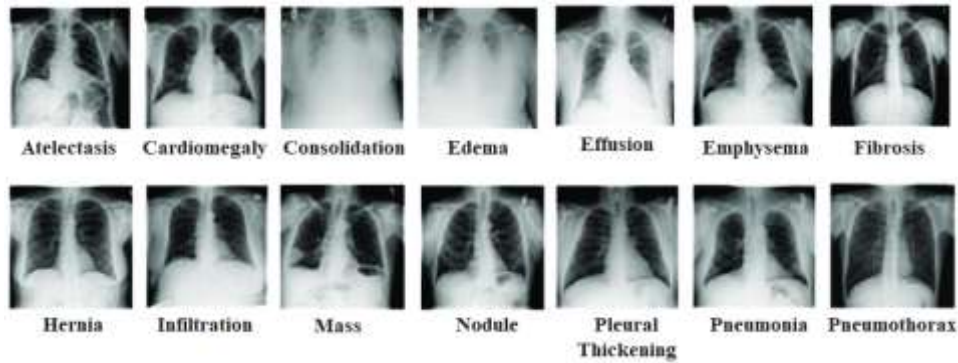


Figure 2. 14 classes of CXR images

2.2. Data pre-processing

The pre-processing must be performed before the feature extraction and classification in lung disease to enhance the performance of the model. The collected CXR data contains noisy data and a class imbalance problem. So, it leads to misclassification problems. Hence in this step, the image denoising and normalization techniques are utilized to enhance the system performance. A detailed explanation of this technique is described in the following subsection.

2.2.1. Image denoising

Usually, the collected CXR image data contains unwanted noises and unclear images, which leads to inaccurate classification results. Hence, image denoising is performed to eliminate the noises from an image to enhance the visual quality. Compared to other filters, the gaussian filter inclines the preserved edges in a lung disease image. Gaussian filter [22] is a smoothing filter, which is utilized for removing the noises from the lung disease image data. In denoising the image, this filter applies the weighted average in the pixel values to minimize the distance from the center pixel value. The gaussian filter supports minimizing the sharp transition edges among the pixels and it makes the images smoother. The denoised image is then provided as input to the normalization process.

2.2.2. Min-max normalization

The collected CXR image dataset involves diverse features with various data ranges. The original feature sets from the CXR take a long convergence rate for training the NN. Hence, the min-max normalization [23] technique is utilized to normalize the input data in the range of 0 to 1 respectively. Normalizing the pixel values ensures that the model can learn effectively from data without being affected by the scale of pixel intensities. The min-max normalization is formulated in (1):

$$X' = \frac{X - X_{min}}{X_{max} - X_{min}} \quad (1)$$

where, X' – normalization data; X – actual data; X_{min} and X_{max} – minimum and maximum data. The min-max normalization is minimally sensitive to the outliers and it enhances the classification results. In this step, the dataset is divided into two parts: 80% of the data are used for the training and 20% images are used for testing. The normalized data is then fed to the feature extraction process to extract the lung image features.

2.3. Feature extraction

In this step, the denoised and normalized CXR images are extracted through the pre-trained CNN architecture. The feature extraction process aims to reduce the high dimensionality of the features and data compaction. In this feature extraction process, the EfficientNetB2 architecture is utilized to extract the lung features. Compared to the other pre-trained models, the EfficientNetB2 architecture accepts the feature maps from previous layers and allows it to reuse the lung image features more effectively. Detailed information about this architecture is provided as subsection below.

2.3.1. EfficientNetB2

The EfficientNetB2 provides the advantage of better-quality features and it effectively simplifies the features in the CXR image. This architecture is usually computationally efficient and obtains greater performance in lung disease classification. The EfficientNetB2 [24], [25] utilizes the compound coefficient to

provide the continuous scaling of width, resolution as well as depth parameters. Every dimension in the image is steadily scaled by the predetermined group of the scaling coefficients. Furthermore, the EfficientNetB2 scales the network breadth, resolution as well as depth of the image by utilizing the group of preset scaling coefficients. The EfficientNetB2 is made up mobile inverted convolutional (MBConv) layer. Based on the various tasks, the network feature in EfficientNetB2 is modified to minimize the number of features as well as ensure enhanced accuracy results. In this feature extractor, the image is provided as input to convolution through a 3×3 convolution kernel and provides the output as a 1×1 convolution layer. The extracted features are then provided to the classification process.

3. CLASSIFICATION

In this stage, the extracted features are provided as input to the classification process to classify chronic lung disease into 14 categories. The DL-based classification approach utilizes the minimum amount of training samples as well as provides superior results. The CNN classifier is utilized for classifying chronic lung disease and detailed information on this classifier is provided in the following subsection.

3.1. Guided backpropagation convolutional neural network

CNN is especially utilized for the classification process, particularly in medical images. The convolution is the mathematical operation that compares the two various functions and it calculates the number of similarity functions. The CNN is made up of three significant layers such as 1 convolution layer, 2 pooling as well as an FC layer. The minimum number of functions in CNN are occupied and compared with every image in the convolutional layer. This procedure developed the feature sets from every input data, generally the dimension is higher than the input data. In this classifier, the input data is provided in the size of $224 \times 224 \times 3$ to the convolutional layer. Assuming that signal P_x and convolute it with the kernel ω , the outcome of this convolution is formulated in (2):

$$(P_x * \omega) = \int P_x(t) \omega(\alpha - t) d\alpha \quad (2)$$

where, $\alpha \in R^n$ for all $n \geq 1$. Now, P_x – input layer of the convolution; output layer is known as the feature-map or activation. Here, in the case of higher dimensions, assuming t as the discrete parameter of the convolution is formulated in (3). In this procedure, α explores the entire values in the space which is not bounded to the specific dimension. I of $m \times m$ pixels are formulated in (4).

$$(P_x * \omega)(\alpha) = \sum_{\alpha} P_x(t) \omega(\alpha - t) \quad (3)$$

$$(I * K)(i, j) = \sum_{p=0}^{m-1} \sum_{q=0}^{m-1} I(p, q) K(1 - p, j - q) \quad (4)$$

At the outcome of the convolution layer, an input image becomes minimally recognizable. Nevertheless, specific data such as orientation, patterns as well as edges in the lung image become more visible. The max-pooling layer is to minimize the size of the feature map without losing a number of helpful data. Between the variants of the pooling operations, max-pooling as well as average-pooling are the most general. The max-pooling as well as average-pooling maintains the larger as well as average value in the CNN. If the max-pooling operation is employed with the kernel size $(p * p)$ as well as the stride of p on $(i * j)$ feature-map, which results in $\left(\frac{i}{p} \times \frac{j}{p}\right)$ feature-map.

Based on the size of the input image as well as the CNN model, the number of convolution as well as pooling layers are utilized. Nevertheless, the feature-map resolution minimizes with every new layer and the machine obtains some relevant features. The FC layer is the final layer of the CNN model, which employs the classification tasks following the principles of the multi-layer perceptron.

GBP is the most utilized method for classification purposes, which provides a visual explanation of the CNN approaches. This GBP approach is a guidance where negative gradients are fixed to 0 through the rectified linear unit (ReLU) activation function in the propagation process. Following this guidance, the GBP denoises the saliency map, making it more effective than other methods of visual explanation approaches. This research applies the GBP in the ReLU activation function and the outcome of this approach is the gradient mask through the pixel. The shortcut connection channel is the variation among the identity x mapping as well as normal CNN, that permits a data estimated from the light convolution layer to straightly attain deep convolution layer. Figure 3 shows the identity mapping module of the CNN.

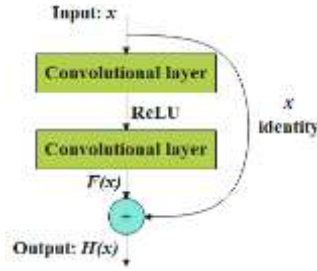


Figure 3. The identity mapping module of CNN

This approach solves a vanishing gradient issue through enhancing the number of convolutional layers as well as enhancing the accuracy of a multi-convolutional layer of the CNN. The outcome of $H(x)$ is converted into $F(x) + x$ is formulated in (5). An arbitrary L-layer feature of the deep neural network (DNN) is acquired through the recursion, which is formulated in (6) and (7) as:

$$H(x) = F(x) + x \tag{5}$$

$$H(x_L) = \sum_{i=1}^{L-1} F(x_i) + x_L \tag{6}$$

$$\frac{\partial Loss}{\partial x_L} = \frac{\partial Loss}{\partial x_L} \left(1 + \frac{\partial}{\partial x_L} \sum_{i=1}^{L-1} F(x_i) \right) \tag{7}$$

Where, x – input; $H(x)$ – an anticipated outcome of basic mapping; $F(x)$ – residual mapping. Optimal learning of mapping target to develop $F(x)$ inclines to 0. $H(x_L)$ – the outcome of l th layer. After that, the Adam optimizer is utilized to identify the discrete learning rate in each parameter for estimating the loss through the categorical loss function. Finally, the data is moved through the ReLU activation function as well and respective classification results are the outcome. The small portions from the predicted outcome are provided to the input layer as a feed to recalculate the weight, so it minimizes the error values and has the faster learning capability to train the model. GBP inclines to overwhelming the inappropriate features as well as noise while focusing on the prominent image parts. This is helpful in lung disease classification, as it supports the network to focus on the appropriate structures within the lung classes. The experimental configurations of the proposed approach are provided in the following section.

4. RESULTS AND DISCUSSION

In this section, effectiveness of the proposed GBPCNN approach is executed on a Python 3.8 environment and the system configuration with Windows 10 OS, Intel Core i7 processor, and 16 GB RAM. The GBPCNN is validated by utilizing various assessment metrics named accuracy, precision, recall, F1-score and area under curve (AUC). The mathematical formula of every metric is described in the following (8)-(12).

$$Accuracy = \frac{TP+TN}{TP+TN+FP+FN} \tag{8}$$

$$Precision = \frac{TN}{TN+FP} \tag{9}$$

$$Recall = \frac{TP}{TP+FN} \tag{10}$$

$$F1 - score = \frac{2TP}{2TP+FP+FN} \tag{11}$$

$$AUC = \frac{\sum R_i(I_i) - I_f(I_i+I)/2}{I_i+I_f} \tag{12}$$

Where, TP - true positive; TN – true negative; FP – false positive; FN – false negative; I_i – number of positive images; I_f – number of negative images; R_i – rate of i th image. Table 1 provides the training hyperparameters of the GBPCNN.

Table 1. Training hyperparameters of the GBPCNN

Hyperparameter	Values
Dimension of an input image	(224, 224, 3)
Kernel size	3 × 3
Batch size	32
Epoch	10
Activation function	ReLU
Optimizer	Adam
Loss function	Categorical loss function

4.1. Performance analysis

The different evaluation metrics are considered for estimating the effectiveness of the proposed GBPCNN approach. The CXR image dataset is utilized to estimate effectiveness of this approach. The proposed method's effectiveness is determined utilizing accuracy and loss function concerning the number of epochs. Tables 2 and 3 show the performance analysis of feature extraction and classification by using CXR image dataset.

Table 2. Performance analysis of feature extraction results

Extractor	Accuracy (%)	Precision (%)	Recall (%)	F1-score (%)
ResNet-50	81.10	80.50	80.00	81.00
VGG16	79.20	75.80	73.40	70.00
DenseNet-121	73.00	72.89	72.65	72.90
EfficientNetB2	97.94	92.00	89.00	92.00

Table 2 shows the EfficientNetB2 with various feature extraction approaches based on the CXR image dataset. The existing feature extraction approaches named ResNet-50, VGG-16, and DenseNet-121 are examined in this section. As compared to these existing approaches, the EfficientNetB2 is effective due to minimizing the number of parameters and operations through utilizing an integration of MBConv and SE blocks in the extraction process. The utilized EfficientNetB2 accomplishes accuracy of 97.94%, precision of 92.00%, recall of 89.00%, F1-score of 92.00% and AUC of 97.94% respectively. The proposed method attains effective outcomes when compared to other extractors with different evaluation indices.

Table 3 shows the GBPCNN with different classifiers for lung disease classification based on the CXR image dataset. The existing classifiers named InceptionV2, VGG-19, and CNN are examined in this section. As compared to these existing approaches, the GBPCNN is effective due to GBP focuses on the affected regions of an input image, so it helps to improve the accuracy of results. The proposed GBPCNN accomplishes an accuracy of 97.94%, precision of 92.00%, recall of 89.00%, F1-score of 92.00% and AUC of 97.94% respectively. The proposed method attains effective outcomes when compared to other classifiers with different evaluation indices. Table 4 shows the analysis of CXR classes using various metrics.

Table 3. Performance analysis of classification results

Classifiers	Accuracy (%)	Precision (%)	Recall (%)	F1-score (%)
InceptionV2	80.05	82.00	80.00	80.00
VGG19	87.90	87.00	87.00	88.00
CNN	74.73	75.00	72.00	73.50
GBPCNN	97.94	92.00	89.00	92.00

Table 4. Analysis of CXR classes using various metrics

Diseases	Accuracy (%)	Precision (%)	Recall (%)	F1-score (%)	AUC (%)
Cardiomegaly	99.89	99.90	98.77	99.90	99.2
Atelectasis	97.11	98.07	97.70	97.00	99.5
Fibrosis	98.47	98.92	98.39	98.50	98.7
Mass	94.25	98.24	98.21	94.50	99.2
Pneumonia	97.23	97.50	97.32	97.30	98.4
Effusion	91.42	98.79	98.27	91.50	99.1
Consolidation	79.01	84.02	83.46	79.00	98.9
Emphysema	93.71	98.90	99.24	93.80	99.4
Edema	88.78	92.88	93.47	89.50	98.8
Infiltration	97.22	99.98	97.01	97.20	99.7
Nodule	70.2	75.04	79.00	78.25	99.6
Pleural thickening	80.62	87.68	87.82	80.70	99.7
Pneumothorax	98.87	99.50	98.70	98.90	99.8
Hernia	91.64	95.15	94.21	91.70	98.9
Average	97.94	92.00	89.00	92.00	97.94

4.1.1. Accuracy function

Figure 4 illustrates the training and validation of the accuracy function for GBPCNN. The accuracy of the validation is attained through the model on the 10th epoch. In the 0th epoch, the training and validation accuracy attains 0.62 and 0.84 respectively. However, in the 9th epoch, the training and validation attain the maximum results of 0.9852 and 0.9794 respectively.

4.1.2. Loss function

Figure 5 represents the training and validation of the loss function for the GBPCNN. The minimum loss of the validation is attained through the model on the 8th epoch, while the training continues until the 9th epoch. But after the 8th epoch, further, the loss was not minimized.

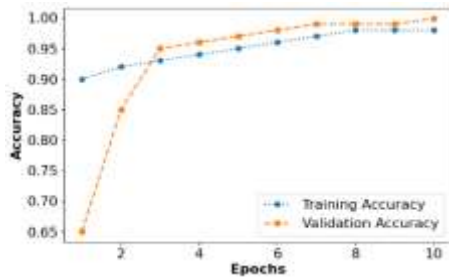


Figure 4. Accuracy function of the GBPCNN

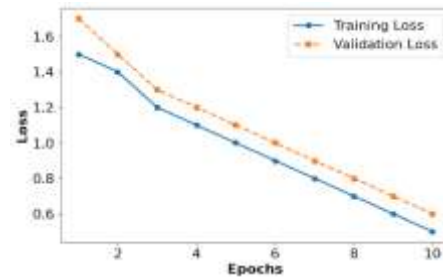


Figure 5. Loss function of the GBPCNN

4.1.3. Confusion matrix

Figure 6 shows the confusion matrix for 14 classes of the CXR dataset. The confusion matrix is estimated with the True class and predicted class. Based on the confusion matrix, the DBPCNN can correctly classify the total of 21,963 images from the testing set of 22,424 images.

4.1.4. ROC curve

Figure 7 shows the confusion matrix for GBPCNN with the affiliation among true positive rate (TPR) as well as FPR. ROC is utilized to represent the estimation of the multi-classification graphically. The receiver operating characteristic (ROC) is one of the famous curves to determine the better classifier and in this process, the area is fixed to 0.72 respectively.

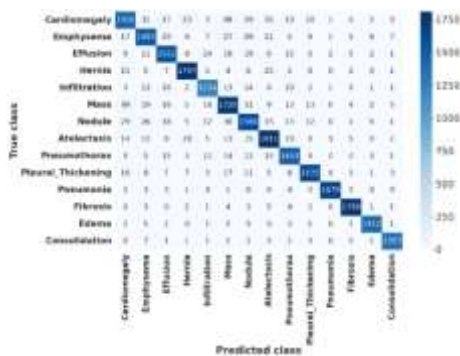


Figure 6. Confusion matrix for 14 classes of CXR dataset

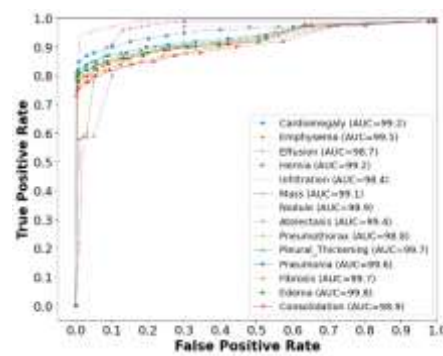


Figure 7. ROC curve of the GBPCNN

4.2. Comparative analysis

Table 5 compares the proposed GBPCNN approach with the existing approaches using different evaluation indices based on the CXR image dataset. The existing methods such as [16]-[19] are compared by utilizing accuracy, precision, recall, F1-score and AUC respectively. The proposed GBPCNN approach attains a high accuracy of 97.94%, precision of 92.00%, recall of 89.00%, F1-score of 92.00%, and AUC of 97.94% respectively.

Table 5. Comparative analysis

Methods	Accuracy (%)	Precision (%)	Recall (%)	F1-score (%)	AUC (%)
MobileLungNetV2 [16]	96.97	96.71	96.83	99.78	N/A
MobileNetV2 [17]	90.2	N/A	N/A	55.6	81.1
A3 Net [18]	N/A	N/A	N/A	N/A	82.6
CX-Ultraneet [19]	88	N/A	N/A	N/A	N/A
Proposed GBPCNN	97.94	92.00	89.00	92.00	97.94

4.3. Discussion

This research provides the step-by-step chronic lung disease framework to improve the classification performance. The proposed GBPCNN approach establishes that it is capable of improving the performance of the system based on the utilization of CXR. The DADCNN enhances the feature representations by producing more informative features on lung disease. Unlike other approaches, GBP localizes the significant features with maximum precision in CNN. In the classification process, the GBP focuses on the particular region with the CXR image to determine the potential lung disease. The proposed DADCNN method is significantly contribute in improving the early diagnosis and treatment of chronic lung cancer, a lead to decreases the mortality rate. The proposed method results align with the scientific consensus on the effectiveness of DL models for medical image analysis. The proposed GBPCNN approach represents a significant advancement in the field of lung cancer diagnosis. The proposed GBPCNN achieves high accuracy and more robust for early detection of chronic lung cancer using CXR. The proposed GBPCNN approach attains a high accuracy of 97.94%, precision of 92.00%, recall of 89.00%, F1-score of 92.00%, and AUC of 97.94% respectively. These results have proven the proposed GBPCNN approach has significantly outperformed well as compared to the previous approaches like MobileLungNetV2 [16], MobileNetV2 [17], A3 Net [18], and CX-Ultraneet [20] respectively. These acquired results represents that the proposed GBPCNN approach effectively distinguishes chronic lung cancer. The proposed approach leverages the GBP to enhance the interpretability of the model, focussing the regions of the CXR images which are most exhibiting of chronic lung cancer.

5. CONCLUSION

This research emphasizes the significance of developing accurate and interpretable diagnostic tools for chronic lung cancer, a leading cause of mortality. In this research, the GBPCNN is proposed for the classification of chronic lung disease into multi-class. Through applying the guided backpropagation in CNN, the approach effectively classifies chronic lung disease by supporting the network to focus on the appropriate structures within the lung classes. The GBP highlights the affected regions of an input image in the classification process. To deal with the stability as well as learning rate of the GBPCNN on the CXR dataset, this approach utilizes the categorical loss function with an Adam optimizer. This approach effectively performs and rapidly detects various lung diseases to enhance the survival rate. As compared to the previous approaches like MobileLungNetV2, MobileNetV2, and CX-Ultraneet, the GBPCNN attains a maximum accuracy of 97.94%. This result highlights the potential of our approach for clinical applications, providing a reliable tool for early detection. The future research will explore integrating the proposed approach with other imaging modalities to enhance overall diagnostic performance. Design experiments with different imaging modalities like CT or MRI to estimate how the data impacts the model's performance and diagnostic accuracy. This research concludes with a take-away statement highlighting the practical implications of the findings. This research significantly contributes to improving chronic lung disease diagnosis and establishes a basis for future advancements.





REFERENCES

- [1] S. Kim, B. Rim, S. Choi, A. Lee, S. Min, and M. Hong, "Deep learning in multi-class lung diseases' classification on chest X-ray images," *Diagnostics*, vol. 12, no. 4, p. 915, Apr. 2022, doi: 10.3390/diagnostics12040915.
- [2] F. M. J. M. Shamrat *et al.*, "LungNet22: a fine-tuned model for multiclass classification and prediction of lung disease using X-ray images," *Journal of Personalized Medicine*, vol. 12, no. 5, p. 680, Apr. 2022, doi: 10.3390/jpm12050680.
- [3] S. Goyal and R. Singh, "Detection and classification of lung diseases for pneumonia and COVID-19 using machine and deep learning techniques," *Journal of Ambient Intelligence and Humanized Computing*, vol. 14, no. 4, pp. 3239–3259, Apr. 2023, doi: 10.1007/s12652-021-03464-7.
- [4] H. Malik, T. Anees, and Mui-zzud-din, "BDCNet: multi-classification convolutional neural network model for classification of COVID-19, pneumonia, and lung cancer from chest radiographs," *Multimedia Systems*, vol. 28, no. 3, pp. 815–829, Jun. 2022, doi: 10.1007/s00530-021-00878-3.
- [5] C. Brestel and M. Cohen-sfaty, "RadBot-CXR: classification of four clinical finding categories in chest X-ray using deep learning," *Medical Imaging with Deep Learning*, no. Midl 2018, pp. 1–9, 2018, [Online]. Available: <https://openreview.net/forum?id=B1tMhcIDM>.





- [6] K. Packhäuser, S. Gündel, N. Münster, C. Syben, V. Christlein, and A. Maier, "Deep learning-based patient re-identification is able to exploit the biometric nature of medical chest X-ray data," *Scientific Reports*, vol. 12, no. 1, p. 14851, Sep. 2022, doi: 10.1038/s41598-022-19045-3.
- [7] V. Ravi, V. Acharya, and M. Alazab, "A multichannel EfficientNet deep learning-based stacking ensemble approach for lung disease detection using chest X-ray images," *Cluster Computing*, vol. 26, no. 2, pp. 1181–1203, Apr. 2023, doi: 10.1007/s10586-022-03664-6.
- [8] V. Ravi, H. Narasimhan, and T. D. Pham, "A cost-sensitive deep learning-based meta-classifier for pediatric pneumonia classification using chest X-rays," *Expert Systems*, vol. 39, no. 7, p. e12966, Aug. 2022, doi: 10.1111/exsy.12966.
- [9] W. M. Salama, A. Shokry, and M. H. Aly, "A generalized framework for lung cancer classification based on deep generative models," *Multimedia Tools and Applications*, vol. 81, no. 23, pp. 32705–32722, Sep. 2022, doi: 10.1007/s11042-022-13005-9.
- [10] A. M. Q. Farhan and S. Yang, "Automatic lung disease classification from the chest X-ray images using hybrid deep learning algorithm," *Multimedia Tools and Applications*, vol. 82, no. 25, pp. 38561–38587, Oct. 2023, doi: 10.1007/s11042-023-15047-z.
- [11] R. Fan and S. Bu, "Transfer-learning-based approach for the diagnosis of lung diseases from chest X-ray images," *Entropy*, vol. 24, no. 3, p. 313, Feb. 2022, doi: 10.3390/e24030313.
- [12] E. Khan, M. Z. U. Rehman, F. Ahmed, F. A. Alfouzan, N. M. Alzahrani, and J. Ahmad, "Chest X-ray classification for the detection of COVID-19 using deep learning techniques," *Sensors*, vol. 22, no. 3, p. 1211, 2022, doi: 10.3390/s22031211.
- [13] V. Ravi, H. Narasimhan, C. Chakraborty, and T. D. Pham, "Deep learning-based meta-classifier approach for COVID-19 classification using CT scan and chest X-ray images," *Multimedia Systems*, vol. 28, no. 4, pp. 1401–1415, Aug. 2022, doi: 10.1007/s00530-021-00826-1.
- [14] S. Sharma and K. Guleria, "A deep learning based model for the detection of pneumonia from chest X-ray images using VGG-16 and neural networks," *Procedia Computer Science*, vol. 218, pp. 357–366, 2022, doi: 10.1016/j.procs.2023.01.018.
- [15] A. A. Abdelhamid, E. Abdelhalim, M. A. Mohamed, and F. Khalifa, "Multi-classification of chest X-rays for COVID-19 diagnosis using deep learning algorithms," *Applied Sciences (Switzerland)*, vol. 12, no. 4, p. 2080, 2022, doi: 10.3390/app12042080.
- [16] F. J. M. Shamrat, S. Azam, A. Karim, K. Ahmed, F. M. Bui, and F. De Boer, "High-precision multiclass classification of lung disease through customized MobileNetV2 from chest X-ray images," *Computers in Biology and Medicine*, vol. 155, p. 106646, 2023, doi: 10.1016/j.combiomed.2023.106646.
- [17] A. Soud, N. Sakli, and H. Sakli, "Classification and predictions of lung diseases from chest x- rays using mobilenet v2," *Applied Sciences (Switzerland)*, vol. 11, no. 6, p. 2751, 2021, doi: 10.3390/app11062751.
- [18] H. Wang, S. Wang, Z. Qin, Y. Zhang, R. Li, and Y. Xia, "Triple attention learning for classification of 14 thoracic diseases using chest radiography," *Medical Image Analysis*, vol. 67, p. 101846, 2021, doi: 10.1016/j.media.2020.101846.
- [19] A. Kabiraj, T. Meena, P. B. Reddy, and S. Roy, "Detection and classification of lung disease using deep learning architecture from X-ray images," in *International Symposium on visual computing*, 2022, pp. 444–455, doi: 10.1007/978-3-031-20713-6_34.
- [20] G. M. M. Alshmrani, Q. Ni, R. Jiang, H. Pervaiz, and N. M. Elshennawy, "A deep learning architecture for multi-class lung diseases classification using chest X-ray (CXR) images," *Alexandria Engineering Journal*, vol. 64, pp. 923–935, 2023, doi: 10.1016/j.aej.2022.10.053.
- [21] "NIH chest X-rays," *www.kaggle.com*. Accessed: Mar., 26 2024. [Online] Available: <https://www.kaggle.com/datasets/nih-chest-xrays/data>.
- [22] M. Rizwan, A. Shabbir, A. R. Javed, M. Shabbir, T. Baker, and D. Al-Jumeily Obe, "Brain tumor and glioma grade classification using gaussian convolutional neural network," *IEEE Access*, vol. 10, pp. 29731–29740, 2022, doi: 10.1109/ACCESS.2022.3153108.
- [23] M. Vedaraj, C. S. Anita, A. Muralidhar, V. Lavanya, K. Balasaranya, and P. Jagadeesan, "Early prediction of lung cancer using gaussian naive bayes classification algorithm," *International Journal of Intelligent Systems and Applications in Engineering*, vol. 11, no. 6s, pp. 838–848, 2023.
- [24] C. Liu, H. Wen, G. Yin, X. Ling, and S. M. Ibrahim, "Research on intelligent recognition method of egg cracks based on EfficientNet network model," in *Journal of Physics: Conference Series*, 2023, vol. 2560, no. 1, p. 012015, doi: 10.1088/1742-6596/2560/1/012015.
- [25] K. Ikromjanov *et al.*, "Region segmentation of whole-slide images for analyzing histological differentiation of prostate adenocarcinoma using ensemble EfficientNetB2 U-net with transfer learning mechanism," *Cancers*, vol. 15, no. 3, p. 762, 2023, doi: 10.3390/cancers15030762.

BIOGRAPHIES OF AUTHORS







Rakesh Selva Raj     has more than 13 years of teaching experience. He is working as Assistant Professor in the Department of ISE, Adichunchanagiri Institute of Technology, Chickmagalur. His research interests include data mining, big data, machine learning, networking, and cloud. He has published papers in international/national conferences and journals. He can be contacted at email: rakeshsr.cseng@gmail.com.



Pavan Kumar Madalu Palakshamurthy     has a Ph.D. from VTU, Belagavi. He has more than 15 years of Teaching experience and has been executing projects in artificial intelligence, machine learning, human behavior analysis, image processing and computer vision. He is currently working as a Professor in the Department of Information Science and Engineering, JNNCE, Shimoga. He is an IEEE senior member and a life member of ISTE. He has various international journal and conference publications with more than 100 citations. He can be contacted at email: pavankumarmp@jnnce.ac.in.



Bidarakere Eswarappa Rangaswamy     presently working as Registrar, Academics, Visvesvaraya Technological University, Belagavi. He was the Dean, Research and Development and Professor and Head at Department of Biotechnology, Bapuji Institute of Engineering and Technology, Davangere. He completed his Masters in 1995 and Ph.D. (2001) from Bangalore University. He has obtained higher level Training in Bacteriology and Air sampling techniques from Environmental Diagnostic Laboratory, Florida, USA in 2008 and attended Course on Aerobiology organized by European Aerobiological Association jointly with International Aerobiology Association (IAA) at Roskilde University Holbaek, Denmark during July 2011. He can be contacted at email: swamyber@hotmail.com.